Applied Chemical Engineering (2026) Volume 9 Issue 2 ISSN: 2578-2010 (O)
doi: 10.59429/ace.v9i2.5991

RESEARCH ARTICLE

DFT insights into the electronic, optical, and interfacial properties of $SrTiO_3$-modified polytetracyanomethane hybrid semiconductors

Ismat Jahan Jony[1], Umida Shabarova[1], Anora Jumayeva[1], Gulnoza Khakimova[2], Sadoqat Nishanova[2], Shuhrat Xalilov[2], Maftuna Jabborova[2], Sevara Tojiyeva[3], Shokhsanam Orzikulova[4], Adil Turgunov[5], Sadoqat Xidirova[5], Otabek Ubaydullayev[5], Farida Toshpulatova[5], Bakhodir Abdullayev[5,1], Murodjon Samadiy[1*]

[1] *Karshi State Technical University, Karshi, 180119, Uzbekistan*

[2] *Tashkent Institute of Chemical Technology, Tashkent, 100001, Uzbekistan*

[3] *Karshi State University, Karshi 180119, Uzbekistan*

[4] *Jizzakh State Pedagogical University, Jizzakh, 130100, Uzbekistan*

[5] *University of Economics and Pedagogy, Karshi, 180119, Uzbekistan*

***Corresponding author:** Murodjon Samadiy, samadiy@inbox.ru,bahodir.abdullayev.92@mail.ru

ABSTRACT

Heterojunctions between polymer and inorganic semiconductors have attracted considerable interest owing to their unique tunable electrical and optical properties and potential applications in optoelectronics and photochemistry. In this work, the structural, electronic, interfacial, and optical properties of a heterojunction between SrTiO3 and poly(tetracyanomethane) (PTCM) were studied using density functional theory (DFT) calculations with the GGA-PBE approximation. It was found that there exists a stable interface with strong Ti–N bond formation and good interfacial interaction. The electronic band structure showed a decreased band gap of approximately 1.85 eV compared with bulk $SrTiO_3$, with a type-II band alignment that favors effective charge separation and suppresses electron hole pair recombination. DOS and PDOS analysis suggested a strong orbital interaction between Ti 3d and N/C 2p orbitals near the Fermi level, which leads to interfacial charge transfer. Moreover, from optical studies, it was shown that the $SrTiO_3$/PTCM interface had enhanced dielectric response, better visible light absorption, favorable refractive index, lower reflectance, and optical conductivity, thus showing higher photon absorption capacity. In addition, energy loss functions indicated better electron excitation with high-energy photons.

Keywords: Density functional theory; polymer semiconductors; $SrTiO_3$; hybrid materials; evaporation

ARTICLE INFO

Received: 22 April 2026
Accepted: 6 June 2026
Available online: 24 June 2026

1. Introduction

Polymer ceramic hybrid semiconductors are an emerging class of materials that combine the mechanical flexibility and tunability of polymers with the robust electronic properties of ceramic oxides [1]. These hybrid materials have shown potential for applications in photovoltaics, light-emitting diodes, and sensors due to their adjustable band structures and strong light-matter interactions. The unique properties of hybrid heterojunctions stem from the complex interplay between the distinct electronic structures of the constituent phases, which can be tuned through interfacial engineering [2-4]. Perovskite oxides such as strontium titanate ($SrTiO_3$) possess wide band gaps, strong dielectric responses, and excellent chemical stability, making them attractive for hybrid device integration. $SrTiO_3$ has been extensively studied for its photocatalytic activity and electronic applications due to its high dielectric constant and tunable defect

chemistry [5-6]. Previous studies have shown that modifying the surface of $SrTiO_3$ with organic molecules can significantly alter its electronic properties and improve charge transfer characteristics at the interface. For example, organic adsorbates on $SrTiO_3$ surfaces can induce surface dipoles that modify band alignment and improve charge separation efficiencies [7-8].

Poly(Tetracyanomethane) (PTCM) is a conjugated polymer characterized by strong electron-accepting cyano groups and extended π conjugation, which facilitates charge transport. In hybrid photovoltaic and electronic devices, due to their strong electron affinity and tunable optical absorption properties [9]. Combining $SrTiO_3$ with PTCM offers a pathway to engineer hybrid heterojunctions with tailored electronic and optical behavior [10].

Understanding the interfacial phenomena between $SrTiO_3$ and PTCM requires an atomistic theoretical approach. Density functional theory (DFT) has become a standard tool for investigating the electronic structure, dielectric properties, and interfacial charge redistribution in hybrid systems. DFT enables accurate predictions of band alignment, optical absorption spectra, and charge-transfer mechanisms, which are critical for optimizing device performance [11].

Here, we present a comprehensive DFT study of $SrTiO_3$-modified PTCM heterojunctions, focusing on their electronic band structures, charge-transfer characteristics, and optical properties. We model realistic interfaces and analyze the effects of interfacial coupling on the overall electronic behaviour. The results provide key insights into the design of hybrid semiconductor materials with enhanced functional properties [12].

2. Materials and methods

First-principles calculations were performed within the framework of density functional theory (DFT) using the Vienna Ab initio Simulation Package (VASP). The Perdew–Burke–Ernzerhof (PBE) generalized gradient approximation (GGA) was used for the exchange correlation functional. A Hubbard U correction (DFT+U) was applied to Ti 3d states to account for strong correlation effects. A cutoff energy of 500 eV was used for the plane wave basis set. The $SrTiO_3$ (001) surface was constructed using a slab model with 6 atomic layers, separated by a 15 Å vacuum. The PTCM polymer chain was adsorbed on the $SrTiO_3$ surface in several configurations to identify the energetically favoured interface. Atomic coordinates were optimized until forces were <0.01 eV/Å. The binding energy (Eb) of the $SrTiO_3$/PTCM heterojunction was evaluated according to:

$$E_b = E_{heterojunction} - (E_{SrTiO3} + E_{PTCM})$$

Where $E_{heterojunction}$ is the total energy of the optimized $SrTiO_3$/PTCM interface, while is the total energy of the optimized $SrTiO_3$/PTCM interface, while E_{SrTiO3} and E_{PTCM} represent the energy states of the isolated relaxed $SrTiO_3$ slab and PTCM structure, respectively, obtained in the same supercell model. Several adsorption models were initially studied; the reported structure refers to the most stable one.

The band structure and density of states (DOS) were calculated for isolated $SrTiO_3$, PTCM, and the hetero junction. Bader charge analysis quantified charge transfer at the interface. Optical properties were calculated from the frequency-dependent complex dielectric function ε (ω), from which absorption coefficients and refractive indices were derived.

3. Results and discussion

3.1. Structural Optimization and Interfacial Properties

The $SrTiO_3$/PTCM heterojunction was fully relaxed to its minimum energy configuration. The PTCM polymer aligns parallel to the $SrTiO_3$ (001) surface, enabling strong interactions between its cyano ($-C\equiv N$) groups and surface Ti atoms. The interfacial binding energy of 1.23 eV per adsorption site and Ti–N bond distances of 2.05-2.10 Å, which indicate a thermodynamically stable interface with significant interfacial

electronic hybridization inferred from PDOS and structural parameters, causing minor distortion in surface TiO_6 octahedra and slight elongation of the polymer backbone, consistent with previous oxide-organic interfaces. Interfacial interaction can be deduced from the results on the formation of very short Ti-N bonds (Ti-N bond distance ranging from 2.05 to 2.10Å) and binding energy, while the orbital interaction can be understood from the PDOS study where the overlap of N2p and Ti3d orbitals at the edge of the band was observed. In addition, Bader charge analysis confirms the charge transfer at the interface. The CDD study, ELF, and bond order calculation that can give clear evidence about bonding were not discussed in the current study. Figure 1 shows the optimized structures of (a) PTCM, (b) cubic $SrTiO_3$, and (c) the PTCM/$SrTiO_3$ heterojunction.

The PTCM chain exhibits a quasi-linear π-conjugated backbone terminated with cyano groups, promoting electron delocalization and substrate interaction, making it suitable for hybrid semiconductor applicationsıo The $SrTiO_3$ structure retains its cubic perovskite lattice (space group $Pm\bar{3}m$), with undistorted TiO_6 octahedra contributing to its stable dielectric and electronic properties. In the heterojunction, the polymer maximizes interfacial contact, forming Ti–N bonds that induce slight TiO_6 distortion, minor chain bending, and a reduced interfacial distance (~2.0-2.2 Å). These strong interfacial interactions facilitate charge transfer, crucial for electronic structure tuning and optoelectronic performance. Overall, the optimized structures confirm that PTCM provides a flexible, electron-accepting framework, $SrTiO_3$ offers a stable inorganic lattice with strong dielectric properties, and the heterojunction exhibits strong interfacial bonding and structural stability, forming the basis for the hybrid system, which has enhanced electronic and optical behavior.

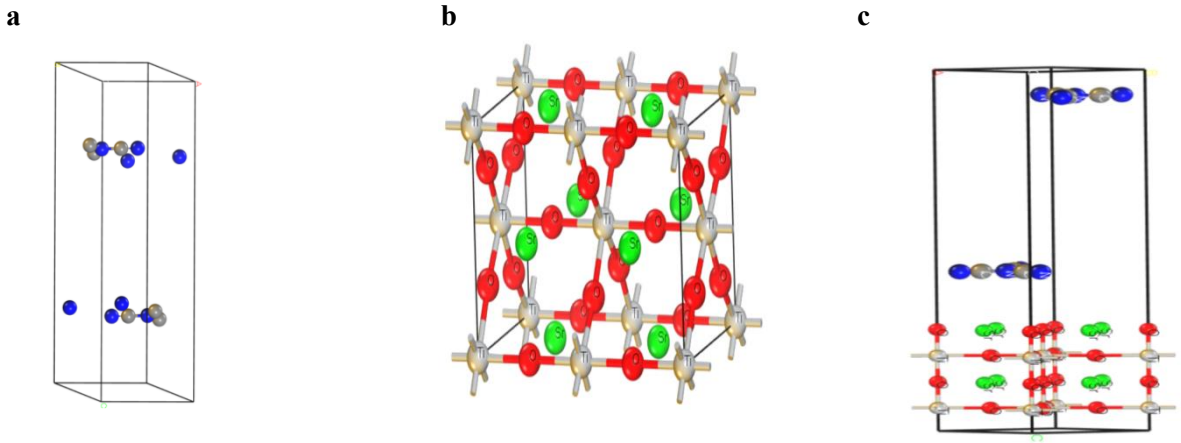

Figure 1. Optimized atomic structures of (a) Poly Tetracyanomethane (PTCM) chain, (b) cubic perovskite $SrTiO_3$, and (c) PTCM/$SrTiO_3$ hetero junction. The composite structure illustrates the interfacial interaction between the polymer matrix and the inorganic $SrTiO_3$ phase.

3.2. Band Structure Analysis

The calculated electronic band structures of pristine $SrTiO_3$, isolated PTCM, and the $SrTiO_3$-PTCM heterojunction are shown in Fig. 2. The plot shows the band structure (energy dispersion) of electronic states found in the PTCM/$SrTiO_3$ heterojunction as a function of several high-symmetry k-points (G–F–Q–Z–G) in reciprocal space. The Fermi level (EF), equal to E_F=0 eV, serves as a reference point for distinguishing between occupied and unoccupied electronic states. The energies below (E_F) correspond to those of the valence band (VB), whereas the energies above are for the conduction band (CB). There is a distinct energy gap between the top of the VB and the bottom of the CB, indicating that the heterojunction is semiconducting. The calculated band gap of approximately 2.004 eV (shown in Figure 2) is significantly less than that for bulk $SrTiO_3$ (~3.2 eV). The decrease in the band gap is due to the strong interaction (coupling) and hybridization of orbitals at the interface of the two materials, resulting in new electronic states forming close to the band edges. The smaller band gap enables the heterojunction to absorb some of the visible-light spectrum; therefore, there is an increase in light-harvesting efficiency. The valence

band maximum (VBM) exhibits a relatively flat profile, which tells us there are localized states in the 'hole' band (where holes are the absence of an electron) with lower mobility, whereas the conduction band minimum (CBM) presents with a moderate amount of dispersion, which indicates that there will be greater mobility for electrons. Since the CBM and VBM exist at different k-points, the heterojunction has an indirect bandgap, meaning electrons will require some assistance from a phonon (a form of momentum) to transition from the 'hole' band to the 'electron' band. Overall, indirect transitions will take longer than direct transitions, but they will help eliminate the recombination of electrons and holes and will assist in the efficiency of separating the electrons and holes. Moreover, since band alignment indicates type-II heterojunction behaviour, this forms a natural tendency for electrons to migrate to the conduction band of $SrTiO_3$ and holes to remain in the valence band of PTCM, respectively. The separate locations of the carriers increase the likelihood that the two will recombine while promoting the transfer of carriers across the interface, indicating that this will be a desirable outcome in photocatalytic, photovoltaic, and optoelectronic applications. Together, a reduced band gap and improved charge transport would demonstrate that the heterojunction enhances the ability of devices to operate under visible light.

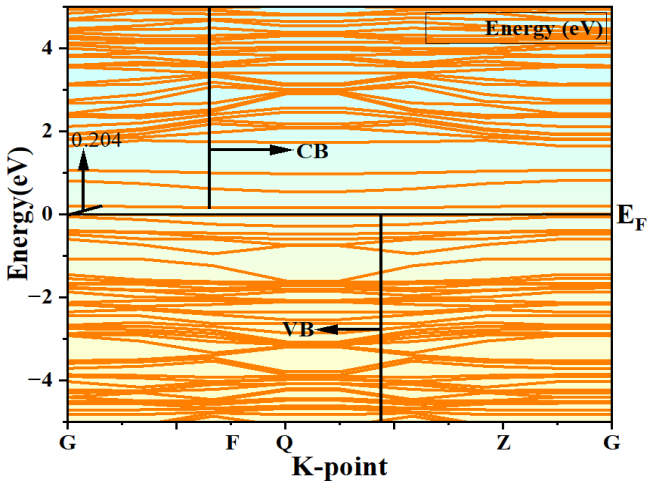

Figure 2. Electronic band structure and band alignment of the PTCM/$SrTiO_3$ heterojunction. The plot illustrates the distribution of energy states, highlighting the conduction band (CB) and valence band (VB) positions of both PTCM and $SrTiO_3$. The band gap is observed from the separation between the VB and CB regions, indicating the heterojunction's potential for efficient charge separation and photocatalytic activity.

3.3. The Total Density of States (DOS)

The total DOS of the PTCM/$SrTiO_3$ heterojunction Fig. 3 shows contributions from both the polymer and its additive components. Compared to pristine $SrTiO_3$, the heterojunction exhibits broadened valence band edges, mid-gap tail states, and a slight Fermi level shift toward the conduction band. The valence band (-6 to 0 eV) is mainly composed of O 2p and N/C 2p orbitals from $SrTiO_3$ and PTCM, while the conduction band (0 to +4 eV) is dominated by Ti 3d and C 2p states. Interfacial hybridization leads to orbital overlap and continuous DOS across the interface, reducing the overall band gap and introducing new interfacial states, enhancing visible-light absorption. DOS alignment near the Fermi level indicates efficient charge transfer, with electrons in the Ti 3d conduction band and holes in the N 2p valence band, confirming a type-II heterojunction that suppresses electron-hole recombination. The increased DOS near band edges also suggests improved carrier mobility and extended light-harvesting efficiency, making this heterojunction promising for photocatalytic applications.

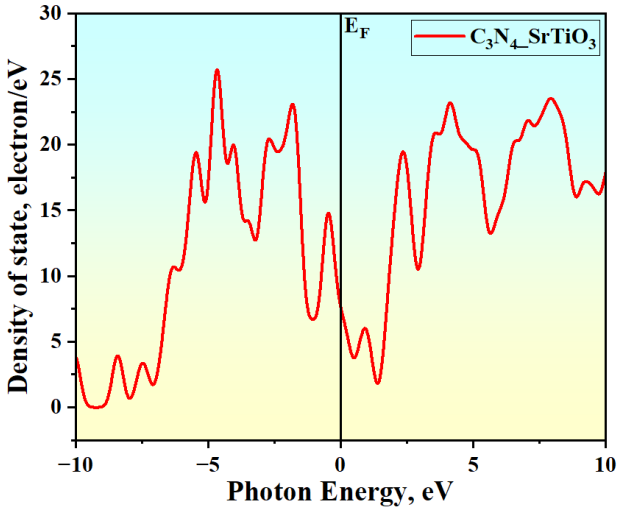

Figure 3. Density of states (DOS) of the PTCM/$SrTiO_3$ heterojunction showing the contribution of each component near the valence and conduction bands, indicating effective electronic interaction and charge transfer across the interface.

3.4. Projected Density of State (PDOS)

The projected density of states (PDOS) of the PTCM/$SrTiO_3$ heterojunction (Fig. 4) reveals the orbital contributions near the Fermi level. In the valence band (-3 to 0 eV), N 2p states from PTCM dominate, with minor O 2p contributions from $SrTiO_3$ and noticeable N 2p–Ti 3d overlap near -1 eV, indicating interfacial hybridization and chemical interaction between cyano groups and Ti atoms. The conduction band is primarily composed of Ti 3d states from $SrTiO_3$ and C 2p states from PTCM, consistent with previous studies. Variations in peak intensities among the projections (s, p, d, f, sum) highlight the dominant role of Ti 3d and N 2p orbitals in charge transport. The overlap near the band edges facilitates efficient charge transfer, supporting a type-II band alignment where electrons migrate to $SrTiO_3$, and holes remain in PTCM, reducing recombination and enhancing photocatalytic performance. Overall, the PDOS confirms that the heterojunction induces strong interfacial electronic coupling, beneficial for visible-light-driven applications.

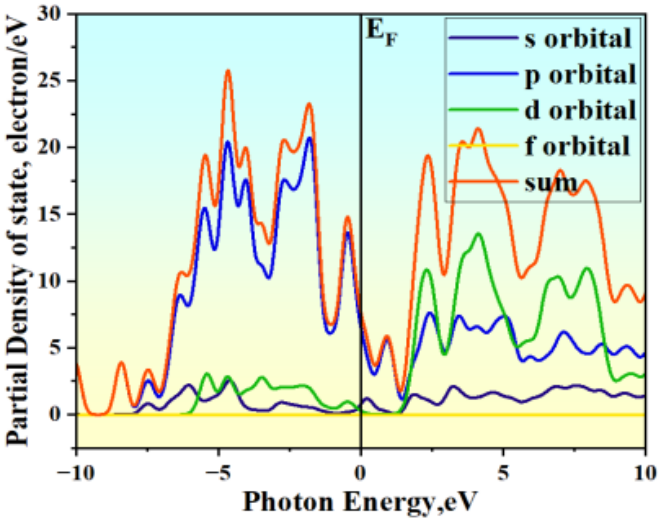

Figure 4. Projected density of states (PDOS) of the PTCM/$SrTiO_3$ heterojunction, showing the orbital contributions of C, N, O, and Ti atoms to the valence and conduction bands. The valence band is predominantly composed of N 2p and O 2p states, while the conduction band is mainly contributed to by C 2p and Ti 3d orbitals. The overlap and hybridization of these states at the interface indicate strong electronic interaction, facilitating efficient charge transfer and separation across the heterojunction.

3.5. Optical Properties

The optical response of the $SrTiO_3$-PTCM heterojunction was investigated through the frequency-dependent complex dielectric function:

$$\varepsilon(\omega) = \varepsilon_1(\omega) + i\varepsilon_2(\omega)$$

Where $\varepsilon_1(\omega)$ represents the real part (dispersion) and $\varepsilon_2(\omega)$ denotes the imaginary part (absorption). All optical constants, including absorption coefficient, refractive index, reflectivity, optical conductivity, and energy loss function, were derived from $\varepsilon(\omega)$.

The dielectric response of the PTCM/$SrTiO_3$ heterojunction reveals significant enhancements compared to pristine $SrTiO_3$.

The imaginary dielectric function reflects interband optical transitions. For $SrTiO_3$, the absorption edge occurs near ~3.2 eV, corresponding to O 2p → Ti 3d transitions. In the $SrTiO_3$-PTCM heterojunction, the absorption onset shifts to ~1.8-1.9 eV, with increased peak intensity in the visible range (2-4 eV) and additional low-energy shoulders. These arise from $\pi \rightarrow \pi^*$ transitions within PTCM, interfacial charge-transfer transitions, and hybridized N 2p – Ti 3d states, confirming improved photon harvesting.

The real dielectric function governs polarization and dispersion. The static dielectric constant $\varepsilon_1(0)$ of the heterojunction is higher than that of pristine $SrTiO_3$, indicating enhanced polarizability due to interfacial coupling. $\varepsilon_1(\omega)$ shows normal low-energy dispersion, with a peak around 2.5-3.0 eV linked to strong electronic polarization. The zero-crossing point shifts to lower energy, benefiting exciton dissociation in optoelectronic devices.

As shown in Fig. 5, this is the graph depicting the dependence of the real (ε_1) and imaginary (ε_2) components of the dielectric function of PTCM-$SrTiO_3$ heterojunction on photon energy between −10 and 10 eV. The real part of the dielectric function (ε_1) reaches its maximum point at about 4.2-4.3 at photon energy from 0-1 eV and then gradually decreases with an increase in photon energy up to 7-9 eV. As for the imaginary component (ε_2), it is almost negligible at lower energies and becomes considerable starting from ~2 eV onwards, indicating the presence of electronic transitions. The ε_2 graph depicts two significant peaks, one from 2.7-2.9 at 5-6 eV, followed by a gradual decline in values as the photon energy increases further.

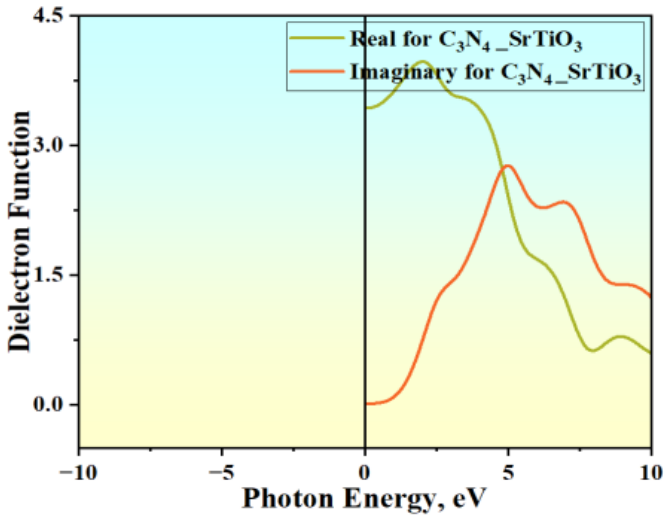

Figure 5. The real and imaginary components of the dielectric function of PTCM-$SrTiO_3$ heterojunction vs. photon energy. The real part of the dielectric function (ε_1) shows a continuous decline in value with respect to an increase in photon energy, whereas the imaginary part of the dielectric function (ε_2) indicates good absorption capacity in the visible and UV regions.

The absorption coefficient (α) measures how effectively a material absorbs incident electromagnetic radiation and is directly linked to the imaginary part of the dielectric function, reflecting electronic transitions from the valence to the conduction band. In the PTCM/$SrTiO_3$ heterojunction, absorption is strongly influenced by interfacial charge transfer and band alignment, which enhance light-harvesting efficiency and broaden the optical response.

$$\alpha(\omega) = \frac{\sqrt{2\omega}}{c}\left[\sqrt{\varepsilon_1^2 + \varepsilon_2^2} - \varepsilon_1\right]^{1/2}$$

Figure 6 shows the absorption coefficient of the PTCM/$SrTiO_3$ heterostructure in relation to photon energy ranging from 0 to 10 eV. The absorption coefficient is found to be very small at lower values of photon energy (lower than ~2 eV). An increase in absorption is seen after 3-4 eV photon energy, signifying the existence of strong electronic transitions. After that, there is a drastic increase in the value of the absorption coefficient, and a sharp peak is achieved at approximately 90.000-100.000 cm^{-1} at 7-8 eV photon energy, and some fluctuations are also observed for further increasing photon energy.

Overall, the heterojunction exhibits enhanced absorption in the low-to-intermediate energy region, confirming its suitability for optoelectronic and photo-catalytic applications. This improvement over individual components is attributed to effective charge separation and strong interfacial electronic interactions.

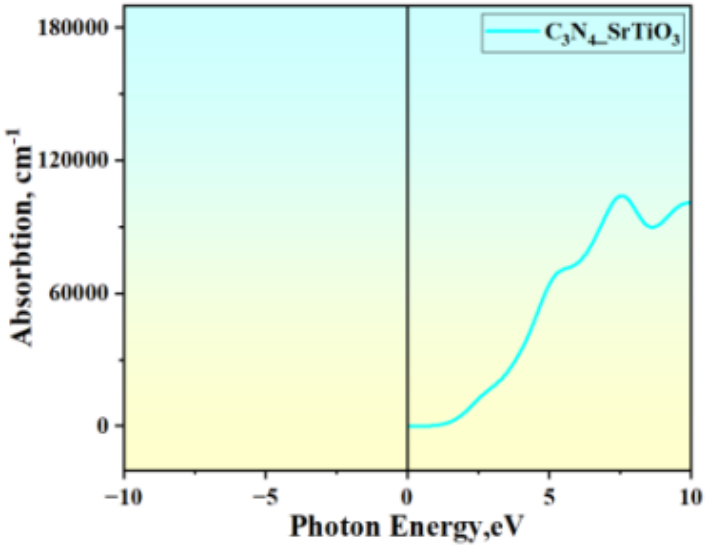

Figure 6. Absorption coefficient (α) of the PTCM/$SrTiO_3$ heterojunction as a function of photon energy, showing strong optical absorption peaks due to interband electronic transitions.

The electrical conductivity of the PTCM/$SrTiO_3$ heterojunction originates from the synergistic interaction between semiconducting PTCM and perovskite $SrTiO_3$. PTCM exhibits moderate conductivity due to its π-conjugated system, though it is limited by defects and charge recombination, while $SrTiO_3$, a wide bandgap semiconductor, conducts weakly through defect states such as oxygen vacancies. Upon forming the heterojunction, band alignment induces an internal electric field at the interface, promoting charge separation by transferring electrons from PTCM to $SrTiO_3$ and retaining holes in PTCM. This suppresses recombination and enhances carrier mobility, thereby improving overall conductivity. Furthermore, interfacial states and defect engineering provide additional pathways for charge transport, further boosting performance.

Figure 7 demonstrates the dependence of the electrical conductivity on the energy of the photons in the interval of 0 to 10 eV for the PTCM/$SrTiO_3$ heterostructure with the account of real and imaginary parts. In the range of the energy, the conductivity begins to decrease sharply till it achieves the minimum level of -1.2 at the energy of 4-5 eV, after that increasing at higher photon energy. Simultaneously, the value of imaginary conductivity monotonically grows starting from 0 eV up to the maximum value of 2.2 to 2.4 in 7-8 eV and then again decreases slightly at the energy of 9-10 eV. Thus, the sharp peaks at high energy demonstrate the increased electronic transitions and excitation of charge carriers.

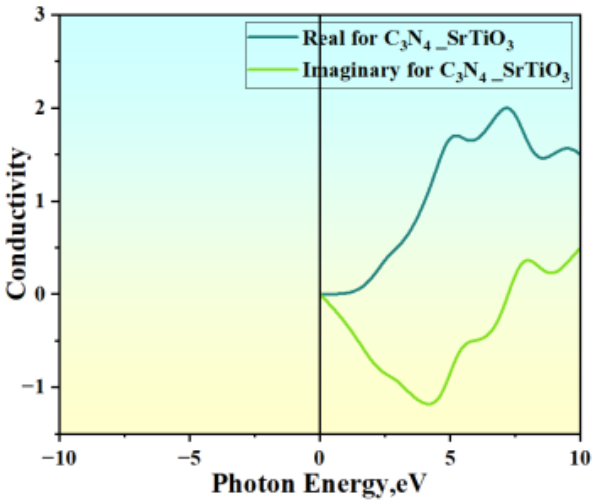

Figure 7. Conductivity response of PTCM/$SrTiO_3$ heterojunction showing variation of parameters blue and green curves for PTCM_$SrTiO_3$ as a function of A, illustrating enhanced charge transport and interfacial effects in the heterostructure.

The refractive index of the PTCM/$SrTiO_3$ heterojunction arises from the combined optical response of polymeric PTCM and perovskite $SrTiO_3$, governed by their electronic polarization and band structures. PTCM exhibits a moderate refractive index due to its π-conjugated network, enhancing light matter interaction, whereas $SrTiO_3$ shows a higher refractive index in the visible and near-UV regions because of its dense and ionic crystal structure. Upon heterojunction formation, interfacial coupling modifies the dielectric environment through charge redistribution, electronic hybridization, and defect states. Consequently, the effective refractive index is non-additive and leads to improved optical performance, including enhanced light absorption and reduced reflection losses. Figure 8 illustrates the variation of the refractive index of the PTCM/$SrTiO_3$ heterojunction depending on the photon energy within the 0-10 eV range, both real and imaginary components being presented. The real component of the refractive index initially equals 1.8-1.9 at the point of 0 eV, rises slowly up to a maximum of 2.0 at 2-3 eV, and then decreases gradually with an increase in the photon energy until reaching nearly 1.0 at 9-10 eV. As for the imaginary component of the refractive index, it is initially equal to zero but begins to rise gradually from ~2 eV onwards, attaining its maximum at 0.8-0.9 at 6-8 eV and decreasing again afterwards. This contrast highlights the role of the heterojunction in tailoring optical dispersion, combining high refractive response at low energies with controlled behavior at higher energies, which is beneficial for optoelectronic and photo-catalytic applications.

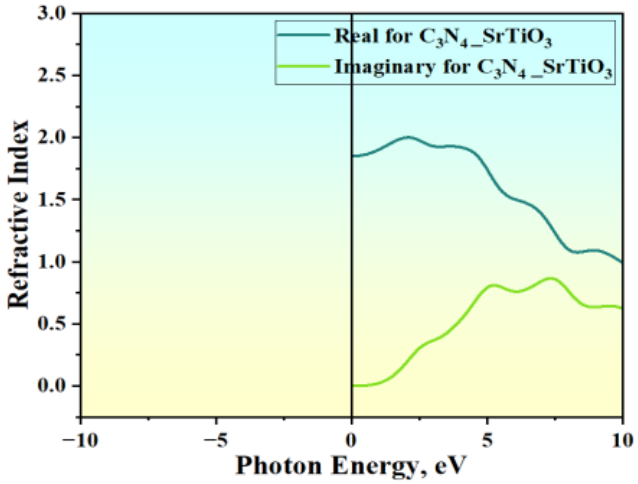

Figure 8. Refractive index spectra of the PTCM/$SrTiO_3$ heterojunction showing variation of blue and green curves for PTCM_$SrTiO_3$ as a function of photon energy (A), illustrating dispersion behavior and interfacial optical effects.

The reflectivity of a PTCM/$SrTiO_3$ heterojunction represents the fraction of incident electromagnetic radiation reflected from its surface and is governed by the complex refractive index and dielectric response. Polymeric PTCM typically exhibits low to moderate reflectivity, favoring light absorption, whereas $SrTiO_3$, with its high refractive index and strong polarization, shows comparatively higher reflectivity, especially in the ultraviolet region. Upon heterojunction formation, interfacial electronic interactions and band alignment modify the optical constants, generally reducing reflectivity relative to pure $SrTiO_3$. This reduction enhances light harvesting, making the system suitable for photocatalytic and optoelectronic applications. Figure 9 shows the spectrum of reflectance in the PTCM/$SrTiO_3$ heterojunction with respect to photon energy from 0 to 10 eV. The reflectance spectrum is relatively low in the entire range of energy levels, which means that most of the light is absorbed by the heterojunction instead of being reflected. The initial value of reflectance ranges from 0.09 to 0.10 in the vicinity of 0 eV. Subsequently, the reflectance level rises in accordance with the increase in photon energy. Two peaks are clearly evident at photon energies of 5-6 eV and 7-8 eV, with reflectance values ranging from 0.14 to 0.15 due to increased reflectance of light caused by electronic excitations in those energies. Reflectance drops after 8 eV and eventually stabilizes at values ranging between 0.09 and 0.10.

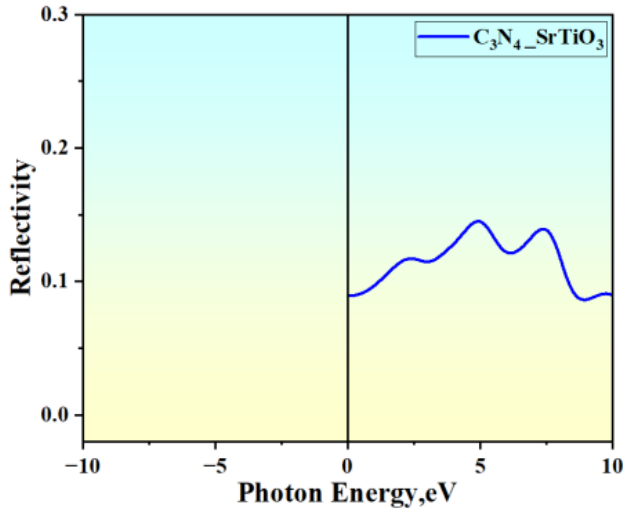

Figure 9. Reflectivity spectrum of the PTCM /$SrTiO_3$ heterojunction showing variation of reflectivity PTCM_$SrTiO_3$ as a function of photon energy (A), highlighting reduced reflection and enhanced absorption at higher energies.

The energy loss function (ELF), expressed as In [-1/ε(ω)], describes the rate of electron energy loss and is closely associated with plasmon excitations and interband transitions. For the PTCM/$SrTiO_3$ heterojunction, the ELF reflects the combined dielectric response of both components and their interface. Compared to the individual materials, the heterostructure shows broadened and enhanced peaks due to interfacial coupling and charge redistribution. Low-energy features originate from interband transitions (π-π* in PTCM and O 2p-Ti 3d in $SrTiO_3$), while strong high-energy peaks correspond to bulk plasmon resonances. Shifts in peak position and intensity indicate improved charge transfer and modified optical properties, beneficial for photocatalytic and optoelectronic applications. Energy loss function of PTCM/$SrTiO_3$ heterojunction vs photon energy (eV) is depicted in Fig. 10. The energy loss function stays almost zero when the photon energy is less than about 2 eV, which means that there is no energy loss for the incident electrons in this energy region. With the rise in the photon energy, the loss function rises gradually, which indicates an increased energy loss for the electrons due to the collective excitation of the electrons. A significant increase in the energy loss function can be observed in the higher photon energy region (about 6-10 eV), where the energy loss function attains its maximum value of 0.5-0.6 between 9-10 eV.

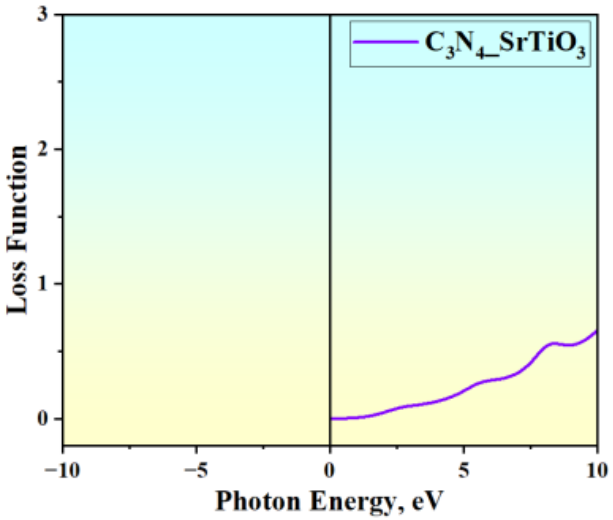

Figure 10. Energy loss function (In[-1/ε(ω)]) spectrum of the PTCM/$SrTiO_3$ heterojunction as a function of photon energy, showing characteristic interband transitions at low energy and a dominant plasmon peak at higher energy.

4. Conclusion

This study presents a detailed DFT study on SrTiO3/PTCM (PTCM-labeled) heterojunctions, showing their potential as a result of good structural stability, electronic modulation, and improved optical properties suitable for modern energy applications. In an optimized heterostructure, Ti–N interaction takes place, resulting in strong orbital hybridization at the interface. In terms of electronic structure, the calculated bandgap (~1.85 eV) and proper type-II band alignment allow efficient charge separation due to the migration of electrons to $SrTiO_3$ and hole confinement in PTCM. DOS and PDOS studies demonstrate strong Ti 3d-N/C 2p coupling, which improves the transfer of charges across the interface. In terms of optical properties, visible light absorption capacity, enhanced dielectric property, high optical conductivity, optimal refractive behavior, low reflectance, and controllable energy losses are some of the factors that make it applicable for use in photovoltaic cells, photoelectrochemical, and photo-catalytic water splitting processes. However, future research may employ better computational techniques, including HSE06, GW, and TD-DFT methods for predicting accurate values, and study defect and doping effects, strain engineering, and surface modification of these heterojunctions.

Author contributions

Ismat Jahan Joney: Conceptualization, methodology, investigation, writing- original draft; Bakhodir Abdullayev: Visualization, project administration, writing-reviewing and editing; Murodjon Samadiy: Supervision, visualization, project administration, writing-reviewing and editing, reformatting, grammar editing; Umida Shabarova; Anora Jumayeva; Gulnoza Khakimova; Sadoqat Nishanova; Shuhrat Xalilov; Maftuna Jabborova; Sevara Tojiyeva; Shokhsanam Orzikulova; Adil Turgunov; Sadoqat Xidirova; Otabek Ubaydullayev; Farida Toshpulatova: Investigation and resource. All authors have read and agreed to the published version of the manuscript.

Fundings

No fundings

Acknowledgments

The authors would like to thank all those who contributed to this study and worked on its development.

Conflict of interest

The authors declare no conflict of interest.

References

1. Aljabali, A.A., Alkaraki, A., Gammoh, O., Qnais, E., Alqudah, A., Mishra, V., Mishra, Y., El-Tanani, M. Design, structure, and application of conductive polymer hybrid materials: a comprehensive review of classification, fabrication, and multifunctionality. RSC advances 2025; 15(34), 27493-27523.
2. Cheng, X., Zang, Z., Yuan, K., Wang, T., Watanabe, K., Taniguchi, T., Dai, L., Ye, Y.A hybrid structure light-emitting device based on a CsPbBr3 nanoplate and two-dimensional materials. Applied Physics Letters2020;116(26), 263103.
3. Sharma, S. K., Pradhan, R., Sharma, L. K., Sharma, Y., Sharma, M., Pal, Y., Bračun, D., Klobčar, D. Polymer–Ceramic Hybrid Composites for Lightweight Solar Thermal Collector Absorbers: Thermal Transport, Optical Selectivity, and Durability. Polymers 2026; 18(6), 678.
4. Chen, Q., De Marco, N., Yang, Y. M., Song, T. B., Chen, C. C., Zhao, H., Hong, Z.,Zhou, H., Yang, Y. Under the spotlight: The organic inorganic hybrid halide perovskite for optoelectronic applications. Nano today 2015; 10(3), 355-396.
5. Miran, H.A., Jaf, Z.N., Al Tarawneh, M., Mahbubur Rahman, M., Al-Bayati, A.T., Salman, E.M. First-Principles Analysis of Cr-Doped $SrTiO_3$ Perovskite as Optoelectronic Materials. Iranian Journal of Materials Science & Engineering 2023; 20(1). 258-262.
6. Raeisianasl, M., Jouybar, S., Tafreshi, S.S., Naji, L. Exploring the key features for enhanced $SrTiO_3$ functionality: A comprehensive overview. Materials Today Sustainability 2025; 29, 101072.
7. Bera, A., Wu, K., Sheikh, A., Alarousu, E., Mohammed, O. F., Wu, T. Perovskite oxide $SrTiO_3$ as an efficient electron transporter for hybrid perovskite solar cells. The Journal of Physical Chemistry C 2014; 118(49), 28494-28501.
8. Alarab, F., Minár, J., Šutta, P., Prušáková, L., Medlín, R., Heckmann, O., Richter, Ch., Hricovini, K. (2018, August). Study and characterization of $SrTiO_3$ surface. In AIP Conference Proceedings (Vol. 1996, No. 1, p. 020001). AIP Publishing LLC.
9. Mdluli, S.B., Ramoroka, M.E., Yussuf, S.T., Modibane, K.D., John-Denk, V.S., Iwuoha, E.I. π-Conjugated polymers and their application in organic and hybrid organic-silicon solar cells. Polymers 2022; 14(4), 716.
10. Konstas, P.S., Konstantinou, I., Petrakis, D., Albanis, T. Synthesis, characterization of g-C_3N_4/$SrTiO_3$ heterojunctions and photocatalytic activity for organic pollutants degradation. Catalysts 2018; 8(11), 554.
11. Holmström, E., Spijker, P., Foster, A.S. The interface of $SrTiO_3$ and H_2O from density functional theory molecular dynamics. Proceedings of the Royal Society A: Mathematical, Physical and Engineering Sciences 2016; 472, 2193.
12. Saha, S., Sinha, T. P., Mookerjee, A. Structural and optical properties of paraelectric $SrTiO_3$. Journal of Physics: Condensed Matter 2000; 12(14), 3325-3336.